Marine Micropaleontology 79 (2011) 41–51

Contents lists available at ScienceDirect

Marine Micropaleontology

journal homepage: www.elsevier.com/locate/marmicro

Research paper

Pleistocene carbonate dissolution fluctuations in the eastern equatorial Pacific on glacial timescales: Evidence from ODP Hole 1241

Joseph J. Lalicata *[,1], David W. Lea

Department of Earth Science, University of California, Santa Barbara, Santa Barbara, CA 93106-9630, USA

ARTICLE INFO

Article history:
Received 1 July 2010
Received in revised form 15 January 2011
Accepted 19 January 2011

Keywords:
eastern equatorial Pacific Ocean
carbonate dissolution cycles
isotope stratigraphy
carbon isotope
benthic foraminifera
lysocline

ABSTRACT

This study presents a record of dissolution from the eastern equatorial Pacific (EEP) that extends to 2.1 Ma, based on sediments from Ocean Drilling Program (ODP) Site 1241. A new benthic oxygen isotope record was developed in order to provide the stratigraphic framework for the Pleistocene section of the core. The isotope record extends back to 2.1 Ma, covering MIS 1–80, and has a sampling resolution of 2 kyr from 0 to 360 kyr and 5 kyr from 360 to 2100 kyr. Dissolution at ODP Site 1241 is characterized through the use of percent coarse fraction (%CF) and shell fragmentation records. These records indicate that %CF in the EEP is recording a dissolution signal dominated by the 41-kyr and 100-kyr climate cycles, and that preservation maxima lag glacial maxima by 9–14 kyr at the major orbital periods. The dissolution signals observed in the ODP Site 1241 record can be correlated across the Pacific and likely record the response to basinwide changes in carbonate chemistry. The dissolution fluctuations and $\delta^{13}C$ signal observed at ODP Site 1241 are consistent with both the Shackleton (1977) and Toggweiler et al. (2006) hypotheses that explain changes in the global carbon cycle during glacial–interglacial transitions.

1. Introduction

1.1. Pleistocene $CaCO_3$ preservation patterns

Deep sea carbonates are one of the largest and most reactive reservoirs for carbon dioxide (Broecker and Peng, 1987). In addition they also provide a record of changes in oceanographic conditions during glacial–interglacial oscillations (Karlin et al., 1992). The amount of carbonate in marine sediments is controlled by the productivity of $CaCO_3$-producing organisms in the surface waters, dilution by terrigenous matter and non-carbonate matter, and the amount of dissolution as the carbonate rains down into corrosive deep waters (Volat et al., 1980). The cause of the Pleistocene calcium carbonate cycles in the equatorial Pacific and their connection to the state of the ocean carbonate system, as well as atmospheric CO_2, have been debated since their discovery (Arrhenius, 1952).

Records of $CaCO_3$ abundance in marine sediments can be correlated across the central and western equatorial Pacific (Farrell and Prell, 1991; Yasuda et al., 1993) and Indian Oceans (Bassinot et al., 1994; Peterson and Prell, 1985), showing that $CaCO_3$ abundance tends to be at a maximum during glacial–interglacial transitions, and at a minimum during glacial onsets. Arrhenius (1952) postulated that a change in the intensity of oceanic and atmospheric circulation during glacial periods caused increased upwelling, and therefore increased $CaCO_3$ productivity. Later studies suggested that enhanced dissolution during interglacial intervals rather than changes in productivity controlled the Pacific $CaCO_3$ cycles; and showed that dissolution consistently lagged oxygen isotope cycles (Berger, 1973; Berger and Johnson, 1976; Ku and Oba, 1978; Le and Shackleton, 1992; Luz and Shackleton, 1975; Matsuoka, 1990; Thompson and Saito, 1974). These observations suggested the Pacific calcium carbonate cycles may be the result of changes in the carbonate ion content of deep waters (Pisias, 1976). The lag between carbonate preservation and sea surface temperature, as represented by the oxygen isotope signal, was suggested to be dependent on the local hydrography of the region (Moore et al., 1977). Other studies examining the cyclic fluctuations in $CaCO_3$ continued to attribute the cyclic features to either dissolution (Anderson et al., 2008; Berelson et al., 1990; Yasuda et al., 1993) or changes in productivity (Adelseck and Anderson, 1978; Archer, 1991; Arrhenius, 1988).

This study presents dissolution records for a relatively shallow water depth core in the eastern equatorial Pacific (EEP), Ocean Drilling Program (ODP) Site 1241 (5°50.570′N, 86°26.676′W; 2027 m). We developed a new stratigraphy for the Pleistocene section of the site based on a benthic oxygen isotope record. Patterns of $CaCO_3$ dissolution in the EEP are compared to other regions in the Pacific in order to determine whether the timing of preservation/dissolution spikes shows a basin-wide signal. These new benthic oxygen and carbon isotope records, as well as the $CaCO_3$ dissolution proxy records are used to test hypotheses explaining Pleistocene dissolution cycles.

* Corresponding author. Tel.: +1 661 665 5399, +1 805 893 8665.
E-mail addresses: jjlalicata@aeraenergy.com (J.J. Lalicata), lea@geol.ucsb.edu (D.W. Lea).
[1] Present Address: Aera Energy LLC, 10000 Ming Ave, Bakersfield, CA 93311, USA.

0377-8398/$ – see front matter © 2011 Elsevier B.V. All rights reserved.
doi:10.1016/j.marmicro.2011.01.002

1.2. Site and core description

Ocean Drilling Project (ODP) Hole 1241 (5°50.570′N, 86°26.676′W) was recovered at a water depth of 2027 m in the Guatemala Basin on Leg 202 of the ODP. The site is located on the sediment-covered north flank of the Cocos Ridge (Cocos Plate) in the EPWP (East Pacific Warm Pool) (Fig. 1). A complete Neogene sediment record was recovered by generating a composite section from splicing together sections of sediment from the three individual holes (~20 m apart) after they had been stratigraphically aligned using magnetic susceptibility data (Mix et al., 2003). The depth scale for the spliced core, adjusted for expansion and contraction is on the corrected meters composite depth (cmcd) scale. Core sediment consists of nannofossil ooze with $CaCO_3$ percentages between 54 and 74%. ODP Site 1241 is located in a tectonically active region with hot spot volcanism characterizing the EEP and volcanism due to subduction occurring on the west coast of Central and South America. Throughout the entire core, seventy-two volcaniclastic horizons were recorded, seventeen of which are in the Pleistocene section (Mix et al., 2003). These ash layers, as well as the newly documented layers from this study, will be of importance when interpreting the carbonate dissolution records in order to distinguish samples that are affected by dilution from non-carbonate sediment.

2. Materials and methods

2.1. Isotope analysis

Isotopic analysis was performed at 5 cm intervals over the top 7.12 cmcd and at 10 cm intervals to 44.96 cmcd. Core material was weighed and disaggregated through a wet-sieving procedure using deionized water to wash and collect the >150 μm fraction of the sample. Samples were allowed to dry for 2 to 3 days before being transferred to vials for picking of individual foraminifer tests. Roughly 10–20 individual shells of the benthic species *Uvigerina auberiana* were weighed, gently crushed, and loaded into Wheaton V-vials. Samples were cleaned prior to analysis as follows: 25 μl of 3% H_2O_2 was pipetted into each vial and left to sit for 30 min in order to purify the samples of organic material. Following the H_2O_2 rinse, samples were ultrasonicated for 2 s in acetone, the supernatant was wicked away, and finally dried in an oven at ~50 °C overnight. Samples were

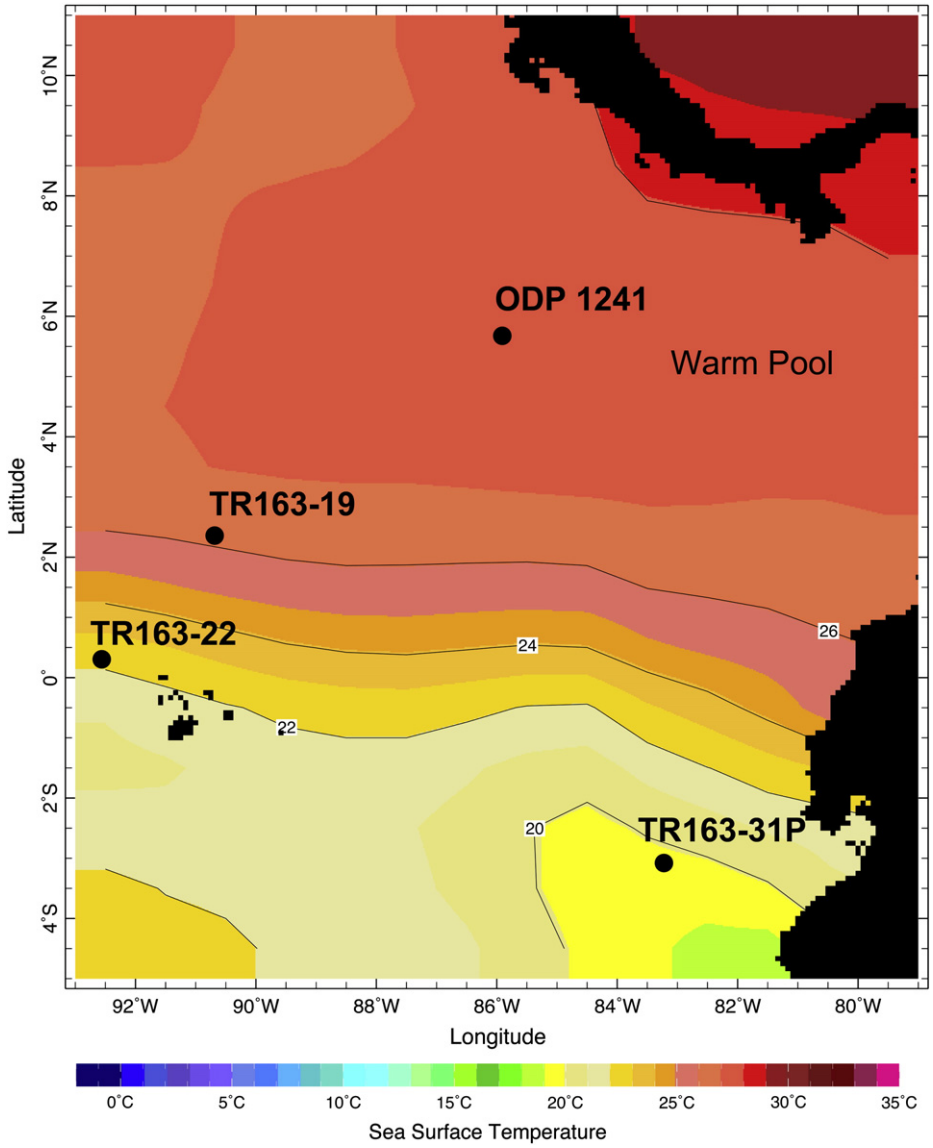

Fig. 1. Locations of cores from the EEP used in this study: ODP 1241 (5°50.570′N, 86°26.676′W, 2027 m water depth), which is the focus of this study, TR163-19 (2°15.5′N, 90°57.1′W, 2348 m water depth), TR163-22 (0°30.9′N, 92°23.9′W, 2830 m water depth), TR163-31P (3°35′S, 83°57′W, 3205 m water depth), and the average annual SSTs in the EEP. While the temperature changes seasonally in the "cold tongue" region (indicated by the black box), temperatures remain relatively stable in the waters around ODP Site 1241. Figure modified from IRI/LDEO Climate Data Library (Reynolds et al., 2002).

then analyzed on a GV Instruments IsoPrime Stable Isotope Mass Spectrometer, with calibration to a house standard, SM92, which was calibrated to VPDB through the NBS-19 standard. Reproducibility of the standard throughout the runs is estimated at ±0.03‰ for $\delta^{13}C$ and ±0.05‰ for $\delta^{18}O$ based on the reproducibility of internal standards.

2.2. Age model

The age model for ODP Site 1241 was developed by tuning the new benthic $\delta^{18}O$ record to the LR04 benthic stack (Lisiecki and Raymo, 2005) using the Match 2.0 software (Lisiecki and Lisiecki, 2002) (Fig. 2). The LR04 stack provides a powerful tool for stratigraphic alignment because it is based on the global mean of variability in 57 globally distributed benthic foraminiferal $\delta^{18}O$ records, therefore increasing the signal-to-noise ratio of the record. Portions of the record with rapid fluctuations in sedimentation rates were eventually used to correctly identify disturbed sections of the core and fine-tune the age model. Visual inspection of the final output from Match 2.0 allowed for the identification of a gap in the composite core (see Section 3.1).

2.3. Carbonate dissolution proxies

Carbonate dissolution fluctuations in ODP Site 1241 were characterized by two proxies: the percent of sediment >150 μm (percent coarse fraction, %CF) and % shell fragmentation (Le and Shackleton, 1992; Yasuda et al., 1993). %CF is the percentage of >150 μm sediment collected in the sieve relative to the whole dry bulk sediment by weight. This method characterizes dissolution because as dissolution intensifies, the walls of the foraminiferal test begin to thin and weaken. These more intensely dissolved tests will break apart into smaller fragments and therefore result in a lower %CF value. %CF was recorded at 5 cm intervals over the top 7.12 cmcd of the core and 10 cm intervals to the base of the core material. Percent shell fragmentation has generally been considered a more robust indicator for carbonate dissolution because it diminishes the influence of other inputs such as terrigenous material, volcaniclastic deposits, and other biogenic inputs that can affect the %CF measurement. Shell fragmentation was measured at 10 cm intervals over the top 3 m of the core using the procedure described in Le and Shackleton (1992): Fragment % = 100*[(# frag/8)/((# frag/8) + (# whole))].

It is important to mention that the %CF proxy can be affected by a number of factors, including dilution by materials other than foraminifera, the occurrence of foraminifera >150 μm (productivity controlled), chemical dissolution of tests, and mechanical destruction of tests. The sediment in the studied interval of core does contain significant amounts of clays (10–20%), as well as sponge spicules, radiolarians, and silicoflagellates contributing <7% (Mix et al., 2003). A few intervals also contain abundant volcaniclastic sediment (Table 2). Variation in these non-carbonate materials will affect the %CF determination. Mechanical destruction, while variable due to the activity of benthic foraminifera and bottom current speed on the sea floor, is related to the intensity of chemical dissolution, as the latter process weakens the foraminiferal tests. The two methods employed in this study are statistically evaluated in order to assess potential pitfalls. Previous studies of sediment cores have compared the results of a number of dissolution proxies (% shell fragmentation, %CF, and *G. menardii* fragmentation index) and have shown agreement in the timing of dissolution cycles (Kimoto et al., 2003; LaMontagne et al., 1996; Le and Shackleton, 1992; Yasuda et al., 1993). We recognize that neither proxies have a simple linear relationship with $CaCO_3$ dissolution, but that the proxies are useful indicators of the relative intensity of dissolution through time.

2.4. Cross-spectral analysis

Cross-spectral analysis was performed between the ODP Site 1241 $\delta^{18}O$, $\delta^{13}C$, and %CF records. Prior to spectral analysis, all records were interpolated to an even 2-kyr time step from 1 to 2100 kyr. Cross-spectral analysis was performed using the Arand software package (Howell et al., 2006) which uses the Blackman–Tukey technique. Iterative cross-spectral analysis was performed on the %CF and isotope records using a window of 400 kyr moving in 200 kyr steps.

3. Results

3.1. Stable isotope stratigraphy and age model of ODP Site 1241

The new oxygen isotope record indicates that the top 45 m of site ODP Site 1241 extends from the late Holocene to marine isotope stage (MIS) 80 at 44.91 cmcd (~2125 kyr) (Fig. 3). The sampling resolution of the record is ~2.1 kyr in the top 7.12 cmcd and is ~5.2 kyr from 7.12 to 44.91 cmcd. Sedimentation rates remain relatively constant throughout the core, varying between ~1.7 cm/kyr and ~2.6 cm/kyr. The average sedimentation rate for the entire sequence is ~2.1 cm/kyr. In the youngest 300–400 kyr of the record sedimentation rates increase slightly to ~2.8 cm/kyr. The average peak-to-peak $\delta^{18}O$ amplitude of interglacial-to-glacial cycles is 1.6‰ in the youngest 400 kyr of the record, decreasing to just less than 1‰ in the oldest 500 kyr of the record. On average $\delta^{18}O$ values between 2.1 and 1 Ma are 0.3‰ more negative than those in the most recent half of the record. Visually inspecting the overlapping isotopic measurements between tie points allowed for graphical manipulation of the depth scale in order to generate a better correlation (corrected tie points listed in Table 1), as well as identification of missing sediment from

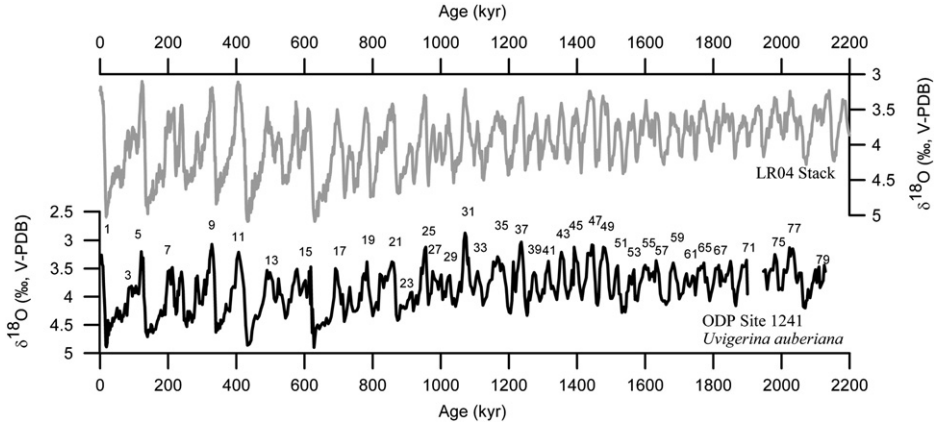

Fig. 2. ODP Site 1241 (5°50.57′N, 86°26.676′W) benthic *Uvigerina auberiana* $\delta^{18}O$ record (bottom) on the new time scale based on visual alignment to the Lisiecki and Raymo (2005) benthic foraminiferal $\delta^{18}O$ stack (top). Marine isotope stages marked on ODP Site 1241 record.

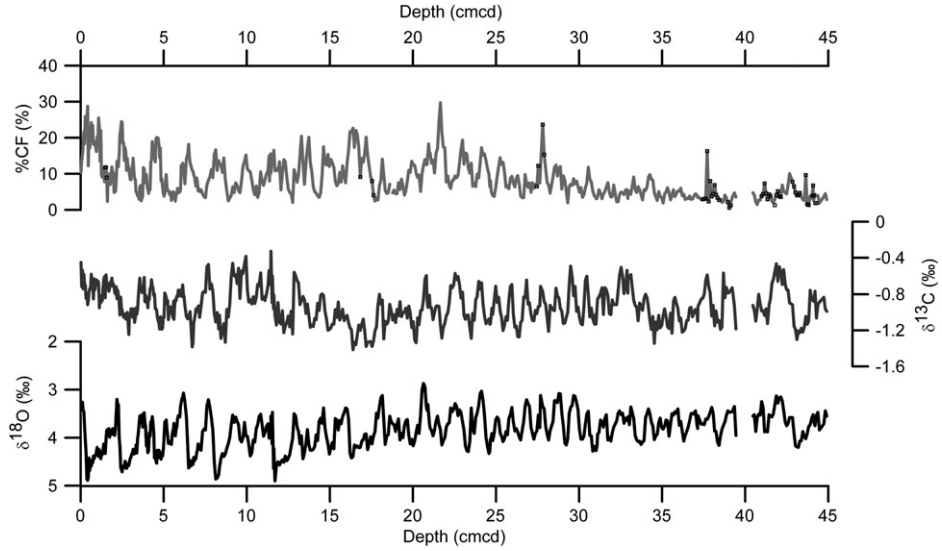

Fig. 3. ODP Site 1241 (5°50.57′N, 86°26.676′W) benthic *Uvigerina auberiana* $\delta^{18}O$ record (bottom), $\delta^{13}C$ record (center), and percent coarse fraction record (%CF) (top) in the depth domain. Depth is on the corrected meters composite scale (cmcd). Sampling resolution is 5 cm intervals in the top ~7.12 cmcd and 10 cm thereafter, with inferred core gap indicated. Squares on the %CF record indicate ash/lapilli layers (Table 2).

the record. MIS 73, representing roughly ~47 kyr of sedimentation, is missing in the composite core (Fig. 4).

The carbon isotope record from ODP Site 1241 is also similar to benchmark records from the region (Fig. 5) (Mix et al., 1995a, b). The most negative values, −1.4‰, occur between 860 and 950 kyr (MIS 21–25). The most positive values, −0.3‰, occur between 450 and 550 kyr in MIS 13–15. The $\delta^{13}C$ and $\delta^{18}O$ records show significant coherence at the major orbital frequencies of 100, 41, and 23 kyr and are in phase throughout the core (Table 3). Core data is available in Appendix A of Lalicata (2009) and will be archived at the NOAA/WDC Paleoclimatology archive.

Table 1
Revised splice tie points, Site 1241.

Hole, core, section, interval (cm)	Depth					Hole, core, section, interval (cm)	Depth			
	(mbsf)	(mcd)	(cmcd)	Age (kyr)			(mbsf)	(mcd)	(cmcd)	Age (kyr)
1241B-1H5W, 25	6.25	6.25	5.53	297.6	Tie to	1241A-2H1W, 123	5.13	6.25	5.53	297.6
1241 C-2H6W, 75	40.25	44.52	39.4	1898.63	Tie to	1241B-5H3W, 72	39.12	44.52	39.4	1898.63

mbsf = meters below sea floor. mcd = meters composite depth. cmcd = corrected meters composite depth.

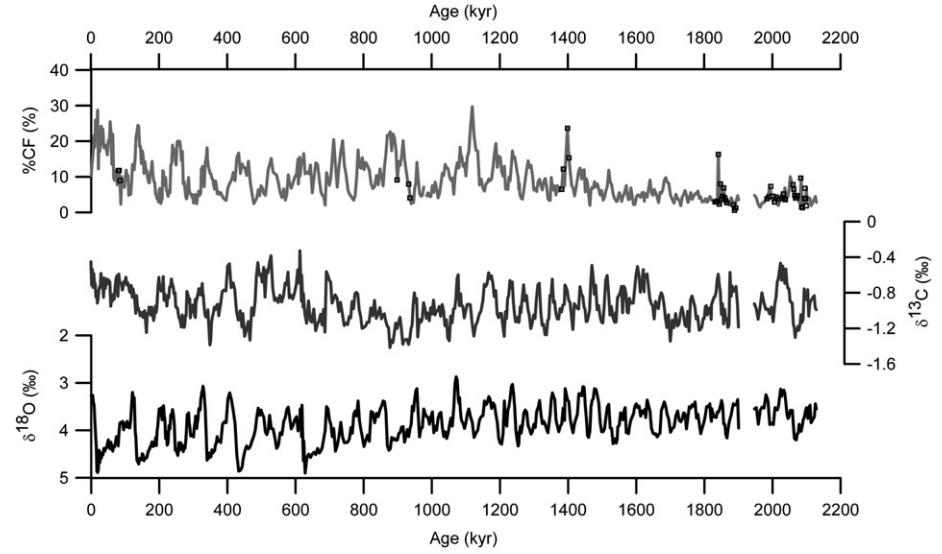

Fig. 4. ODP Site 1241 (5°50.57′N, 86°26.676′W) benthic foraminiferal *Uvigerina auberiana* $\delta^{18}O$, $\delta^{13}C$, and %CF records on an age scale based on alignment to the Lisiecki and Raymo (2005) benthic foraminiferal $\delta^{18}O$ stack. Phase analyses on the records indicate that $\delta^{18}O$ and $\delta^{13}C$ are in phase. Preservation maxima (high %CF) lag glacial maxima by 9–22 kyr on the orbital frequencies. Squares on the %CF record indicate ash/lapilli layers (Table 2).

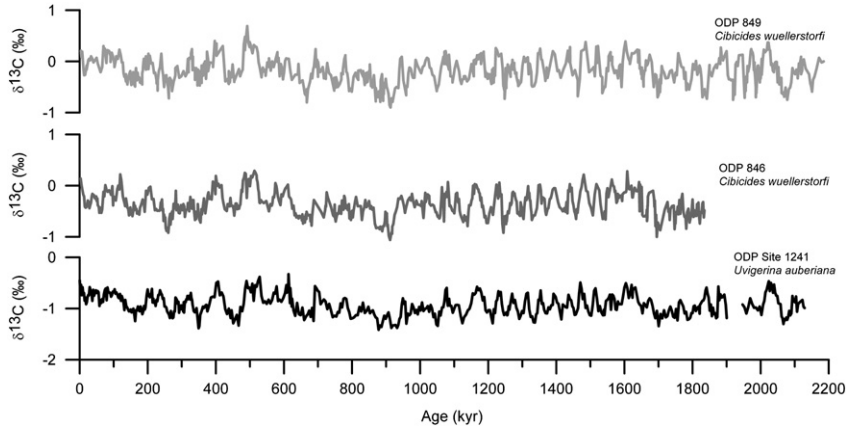

Fig. 5. ODP Site 1241 (5°50.57′N, 86°26.676′W) *Uvigerina auberiana* $\delta^{13}C$ record (bottom), compared with *Cibicides wuellerstorfi* $\delta^{13}C$ records from EEP sites ODP 846 (center) (3°5.7′S, 90°49.1′W) (Mix et al., 1995a) and ODP 849 (top) (0°11′N, 11–°31.1′W) (Mix et al., 1995b). Sample resolution for ODP Site 1241, ODP 846, and ODP 849 is 10 cm. Comparison of the records shows that ODP Site 1241 is in agreement with other benchmark records and is, on average, more negative due to species specific offsets between *U. auberiana and C. wuellerstorfi* (Shackleton and Hall, 1984).

3.2. $CaCO_3$ dissolution data

The %CF and % shell fragmentation records display a strong correspondence, with a cross correlation r = 0.78 (Fig. 6). Percent fragmentation values range from a maximum of 20% at 89.5 kyr to a minimum of 4.8% at 63.3 kyr. At the core top, values for % shell fragmentation and %CF are 19.4% and 10.4%, respectively. The core top values indicate a sharp increase in dissolution from the preservation maximum at ~14 kyr and ~19 kyr, where % shell fragmentation is 6% and %CF is 28.7% respectively.

The %CF record displays a cyclicity that is somewhat similar to the $\delta^{18}O$ record, with higher frequency cycles superimposed on longer 100 kyr cycles (Fig. 4). Between 2100 and 1300 kyr the %CF values remain relatively constant. Between 1300 and 1100 kyr %CF values begin to fluctuate with larger amplitudes. The average value for %CF is 6% between 2100 and 1100 kyr, increasing to 11% between 1100 and 0 kyr. Values fluctuate from maxima of 20–24% to minima of 2–3% between 200 and 0 kyr. From 1100 to 800 kyr, %CF maxima are above 20%, with the highest value in the record (~30%) occurring at 1118 kyr. From 700 to 400 kyr, %CF maxima are lower and do not exceed 15–17%.

Cross-spectral analysis was performed between the %CF, $\delta^{18}O$, and $\delta^{13}C$ records (Table 3). The %CF record lags the $\delta^{18}O$ and $\delta^{13}C$ records. Cross correlation between the %CF record and $\delta^{18}O$ has r-values averaging 0.81 between 1 and 950 kyr and 0.7 between 950 and 1800 kyr. Between 1 and 950 kyr, the %CF and $\delta^{18}O$ records show significant coherence at the 95% confidence interval for the 100 and 41 kyr orbital periods and 80% confidence interval for the 23 kyr orbital period, with preservation maxima lagging ice volume maxima by 8.9 ± 2.5 kyr at the 23 and 41 kyr orbital frequency and 14.4 ± 3 kyr at the 100 kyr frequency. Between 950 and 1800 kyr the %CF and $\delta^{18}O$ records show significant coherence at the 95% confidence interval for the 41 and 23 kyr orbital periods, with preservation maxima lagging ice volume maxima by 14.1 ± 2.6 and 10.6 ± 1.7 kyr at the 41 and 23 kyr orbital periods, respectively. Overall cross correlation between %CF and $\delta^{18}O$ for ODP Site 1241 is r = 0.64, with an overall lag of 12 kyr for %CF to achieve maximum correlation. Correlation between the %CF record and $\delta^{13}C$ record averages r = 0.79 between 1 and 950 kyr and r = 0.5 between 950 and 1800 kyr. Between 1 and 950 kyr, the %CF and $\delta^{13}C$ records show significant coherencies at the 100 and 41 kyr orbital periods, with preservation maxima lagging $\delta^{13}C$ maxima by 19 ± 5.6 kyr and 9.3 ± 3 kyr respectively. Between 950 and

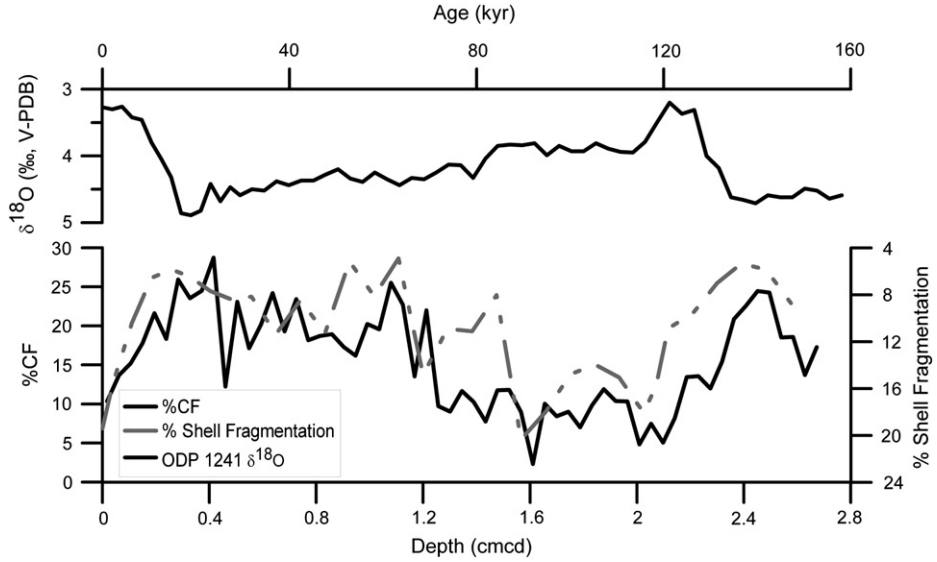

Fig. 6. ODP Site 1241 (5°50.57′N, 86°26.676′W) %CF record compared with shell fragmentation record. Visual inspection of the relationship between the two records suggests dissolution is the dominant influence on the %CF record. The correlation between the two data series is r = 0.78.

1800 kyr, the %CF and $\delta^{13}C$ records show significant coherencies at the 100, 41, and 23 kyr orbital periods, with preservation maxima lagging $\delta^{13}C$ maxima by 15.4 ± 6.5, 12.6 ± 1.8 and 6.5 ± 1.5 kyrs, respectively.

4. Discussion

4.1. %$CaCO_3$ and dissolution records

The % shell fragmentation and %CF records are ultimately only proxies for the intensity of dissolution. The %$CaCO_3$ record from ODP Site 1241 varies from 54.4 to 77.8% over the studied intervals with an average of 66.2% (Mix et al., 2003). It is difficult to evaluate the dissolution proxies presented in this paper in relation to the %$CaCO_3$ record for ODP Site 1241 (Mix et al., 2003) because the %$CaCO_3$ record has a coarse sampling resolution of ~1–2 m and does not allow for a rigorous comparison between the data sets. A study of a central equatorial Pacific Ocean core by LaMontagne et al. (1996) compared three dissolution proxies to the record of $CaCO_3$ concentration. The use of three different dissolution proxies (% shell fragmentation, the foraminiferal dissolution index (Vincent and Berger, 1981), and the relative abundance of benthic foraminifera to total foraminifera) allowed for the mitigation of any sampling/handling artifacts associated with each method. Their study concluded that the data for the three dissolution proxies, while in phase with each other and strongly lagging the glacial maxima at the 100 kyr frequency, were unrelated to the concentration of $CaCO_3$. It was also observed that there were episodes in which high concentrations of $CaCO_3$ were coincident with relatively poor foraminiferal preservation and vice versa (LaMontagne et al., 1996). Although the resolution of the data from ODP Site 1241 precludes a direct comparison of %$CaCO_3$ and the dissolution indices presented in this study, the LaMontagne et al. (1996) study shows that there may not exist a linear relationship between dissolution proxies and the concentration of $CaCO_3$ and that methods such as %CF and % shell fragmentation may be the only way to qualitatively examine fluctuations in dissolution intensity.

4.2. Carbonate dissolution and the $\delta^{13}C$ record

To determine whether changes in the intensity of dissolution or other factors are controlling the %CF record from ODP Site 1241, the %CF record was compared to shell fragmentation measurements in the top ~3 m of the core (Fig. 6). Le and Shackleton (1992) demonstrated that as dissolution intensifies, foraminifera tests weaken, therefore becoming more susceptible to fragmentation by various mechanical processes on the seabed. The correlation between the two records is relatively strong (r = 0.78) and suggests that dissolution is the dominant control on %CF during glacial to interglacial changes. It is important to note that ODP Site 1241 is located in a tectonically active region, and due to its proximity to the Galápagos hot spot and Central/South America, the %CF record is influenced by ash layers (Mix et al., 2003). The ash and lapilli layers are usually isolated to a single 5–10 cm interval and therefore can be taken into consideration when interpreting and describing the %CF record. Ash layers in the %CF record are marked on Figs. 3 and 4 and ages of the most abundant ash occurrences are listed in Table 2. The frequency at which ash layers occur in the sediment core is notably higher between 1.8 and 2.1 Ma BP, with 14 samples containing ash between 1831 and 1891 kyr and 19 samples containing ash between 2026 and 2104 kyr. It is important to note that these may not all be individual volcanic events as some of these ash occurrences may be continuous layers.

4.3. Dissolution at ODP Site 1241 compared to other EEP cores

Visual comparison of the %CF record from ODP Site 1241 to %CF records from three previously studied EEP cores (TR163-19, TR163-22, and TR163-31P), which span 130–360 kyr BP, shows a correlation in the timings of the major spikes in preservation (Fig. 7), particularly a large preservation spike at ~14 kyr that has been observed as a global event (Berger, 1977). A second major preservation spike readily visible in the region occurs at 136–140 kyr. The record from TR163-19 (2°15.5′N, 90°57.1′W; 2348 m) shows the most similarities with ODP Site 1241, which is expected because they both lie on the Cocos Ridge. The %CF values in TR163-19 are generally greater than at ODP Site 1241, an unexpected observation given that TR163-19 is at a deeper water depth (2348 m vs. 2027 m), and the solubility of calcite increases with water depth and pressure. This difference in preservation may be the result of the higher sedimentation rate, ~3 cm/kyr, at TR163-19 (Lea et al., 2000), as compared to the sedimentation rate of ~2.1 cm/kyr at ODP Site 1241. The effect that water depth has on the intensity of dissolution may be overprinted by this difference in sedimentation rates because $CaCO_3$ sediments raining down from the surface will spend less time in corrosive deep waters before being buried. Although the difference in preservation may be affected by the sedimentation rates, another possibility may be the difference in susceptibility to dissolution between faunal assemblages at the two sites (Berger, 1970). Berger (1970) demonstrated that certain species of foraminifera are more susceptible to dissolution than others. Foraminifera that are more prone to dissolution, such as *Orbulina universa*, may inhabit the year-round warmer waters of ODP Site 1241, and therefore %CF values may be lower because of preferential

Table 2
Major volcaniclastic layers in composite section, Site 1241.

Hole, core, section	Interval (cm)	(cmcd)	Age (kyr)	Visual description
1241B-1H2W	16–18	1.31	79	Clear-brown glass
1241B-1H2W	21–23	1.35	82	Clear-brown glass
1241B-1H2W	26–28	1.39	85	Clear-brown glass
1241A-3H3W	86–88	14.90	898	Clear-brown glass
1241A-3H4W	16–18	15.52	932	Clear glass
1241A-3H4W	26–28	15.60	935	Orange glass shards
1241A-4H3W	116–118	24.30	1382	Pumice (lapilli)
1241A-4H3W	126–128	24.38	1386	Pumice (lapilli)
1241A-4H4W	6–8	24.61	1398	Pumice (lapilli)
1241A-4H4W	16–18	24.69	1403	Clear-brown glass
1241C-2H5W	6–8	33.14	1831	Black ash
1241C-2H5W	16–18	33.22	1834	Small pumice
1241C-2H5W	26–28	33.30	1838	Black ash
1241C-2H5W	46–48	33.46	1844	Pumice (lapilli)
1241C-2H5W	56–58	33.53	1847	Pumice (lapilli)
1241C-2H5W	66–68	33.61	1850	Black ash
1241C-2H5W	76–78	33.69	1853	Ash and pumice
1241C-2H5W	86–88	33.77	1857	Ash and pumice
1241C-2H5W	96–98	33.85	1860	Pumice (lapilli)
1241C-2H5W	106–108	33.93	1863	Pumice (lapilli)
1241C-2H5W	116–118	34.00	1866	Pumice (lapilli)
1241C-2H6W	26–28	34.47	1885	Black ash
1241C-2H6W	36–38	34.55	1888	Clear glass
1241C-2H6W	46–48	34.63	1891	Clear glass
1241B-5H5W	36–38	36.98	2026	Clear glass and pumice
1241B-5H5W	46–48	37.06	2029	Clear glass and pumice
1241B-5H5W	66–68	37.22	2035	Clear glass and pumice
1241B-5H5W	76–78	37.29	2038	Clear glass and pumice
1241B-5H6W	6–8	37.92	2060	Pumice (lapilli)
1241B-5H6W	16–18	38.00	2063	Pumice (lapilli)
1241B-5H6W	26–28	38.08	2065	Pumice (lapilli)
1241B-5H6W	36–38	38.15	2068	Pumice (lapilli)
1241B-5H6W	46–48	38.23	2070	Pumice (lapilli)
1241B-5H6W	56–58	38.31	2073	Pumice (lapilli)
1241B-5H6W	96–98	38.62	2083	Pumice (lapilli)
1241B-5H6W	106–108	38.70	2085	Black ash
1241B-5H6W	116–118	38.78	2088	Black ash
1241A-6H1W	36–38	38.98	2094	Clear-brown glass
1241B-5H6W	146–148	39.02	2095	Clear-brown glass
1241A-6H1W	46–48	39.06	2097	Pumice (lapilli)
1241A-6H1W	56–58	39.13	2099	Pumice (lapilli)
1241A-6H1W	66–68	39.21	2102	Clear-brown glass
1241A-6H1W	76–78	39.29	2104	Clear-brown glass

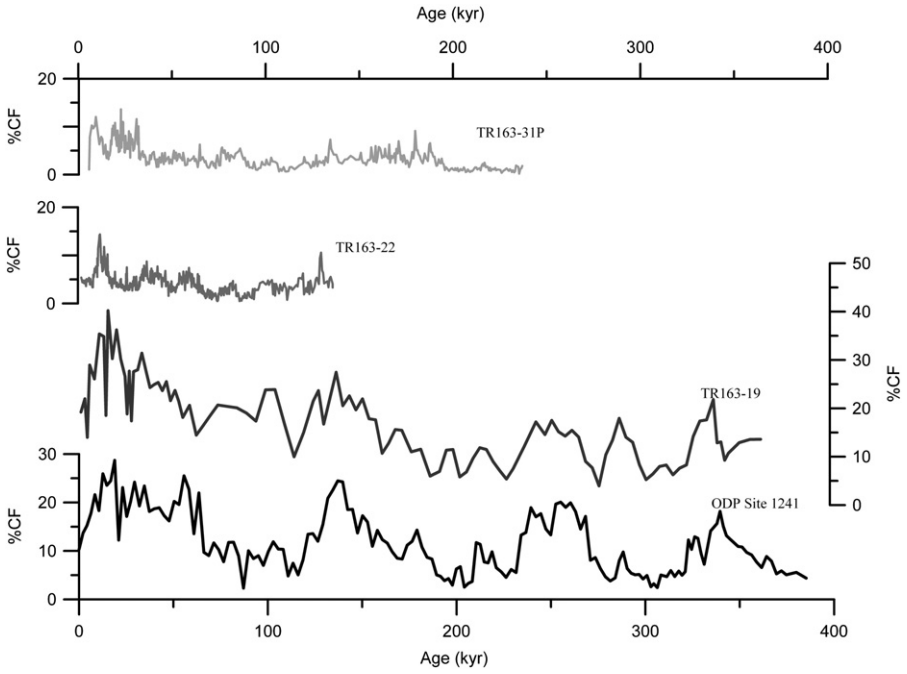

Fig. 7. %CF records from available EEP cores (all axes on the same scale): ODP Site 1241 (5°50.57′N, 86°26.676′W; 2027 m) (bottom), TR163-19 (2°15.5′N, 90°57.1′W; 2348 m) (bottom center) (Lea et al., 2002), TR163-22 (0°30.9′N, 92°23.9′W; 2830 m) (Lea et al., 2006), and TR163-31P (3°35′S, 83°57′W; 3205 m) (Martin et al., 2002). Visual agreement between three of the cores indicates the presence of a regional dissolution signal. All records show a preservation spike at ~14 and ~130 kyr. The record from TR163-31P does not correlate as well due to input from terrigenous material.

dissolution of these species. The %CF record from TR163-22 (0°30.9′N, 92°23.9′W; 2830 m) shows similar timings for the dissolution fluctuations, but the preservation is much poorer at this deeper site (2830 m). Although the average sedimentation rate at TR163-22 is 7 cm/kyr, increased calcite solubility due to greater depth (pressure) appears to be the dominant factor influencing preservation. Preservation of carbonate sediment at TR163-31P (3°35′S, 83°57′W; 3205 m) is comparable to TR163-22, which would be expected because it has a similar sedimentation rate (~7 cm/kyr) and a water depth of 3205 m. The %CF record from TR163-31P, which is punctuated by intervals of anomalously high %CF values, appears to be the only record that does not show the same general fluctuations in %CF for the top 50 kyr. These high %CF intervals are due to input of terrigenous matter, and visual inspection of the core material confirms the presence of non-$CaCO_3$ sediment (Martin et al., 2002). When these samples are filtered out of the %CF record, there is agreement with the other cores in that maximum preservation (maximum %CF) occurs during glacial to interglacial transitions. The similarities shared between the %CF records from the EEP indicate that a regional dissolution signal is reflected in the records.

An interesting observation in the comparison of the %CF records from the EEP is that the magnitudes of fluctuations are markedly different between the shallow water cores (TR163-19 and ODP Site 1241) and the deeper water cores (TR163-31P and TR163-22). The modern day lysocline in the Panama Basin, just east of our study site, is estimated to be just below ~2900 m (Thunell et al., 1981), and during the most intense periods of dissolution most likely never shoaled above ~2900 m (López-Otálvaro et al., 2008). So although dissolution is occurring above the lysocline, this observation would seem to rule out the possibility that differences in the magnitudes of dissolution fluctuations were the result of a shifting lysocline that caused greater dissolution in shallower cores than deeper cores. These variations may be the result of productivity changes between glacial and interglacial periods (Adelseck and Anderson, 1978; Archer, 1991; Arrhenius, 1988; Murray et al., 2000), yet studies have disagreed as to whether there have been significant changes in EEP productivity (Anderson et al., 2008; Luz and Shackleton, 1975; Paytan et al., 1996; Pedersen, 1983). Berger (1973) suggested that intensity of carbonate dissolution was the dominant control on the observed carbonate cycles in deep cores near the lysocline, but that $CaCO_3$ records could also be influenced by productivity fluctuations. Based on measurements from shallow and deep EEP cores, Adelseck and Anderson (1978) proposed two means in which productivity may affect carbonate fluctuations: a change in productivity resulting in increased deposition and/or a change in the amount of planktonic foraminifers resistant to dissolution.

The suite of cores presented in Fig. 7 represents deeper waters near the lysocline and shallower waters in areas of the EEP that are located in the productive upwelling zone, as well as just slightly north of those waters. Since the major preservation spikes at ~14 and ~136–140 kyr are visible in all the cores in very different productivity regimes, changes in dissolution intensity are likely a regional control on %CF. In order to more clearly see the magnitude of the fluctuations throughout the four cores, %CF values were normalized to between 0 and 1 (Fig. 8). The normalized values reveal that the relative fluctuations do not appear to be markedly different between the shallow- and deep-water cores. The productivity factors described by Adelseck and Anderson (1978) may influence these sites, but TR163-19 and ODP Site 1241 may be too far north of the productive upwelling zone to be affected by large changes in productivity. Murray et al. (2000) examined the interrelationship between regional productivity variations and dissolution influences on the concentration of sedimentary carbonate in a north to south transect of cores from the central equatorial Pacific Ocean. They show that across all latitudes studied (4°N–5°S), glacial climatic states generally have greater export production, with maxima in export occurring during glacial transitions. The higher latitude cores record minimal absolute export changes during glacial-to-interglacial cycles, whereas at the equator export productivity changes dominate. Should the same conditions apply to the EEP, ODP Site 1241, located at 5°N, is at a latitude at which carbonate concentration records are dominated by dissolution rather than export production (Murray et al., 2000). TR163-19, TR163-22, and TR163-31P are located at 2°N, 0°N, and 3°S respectively, and therefore

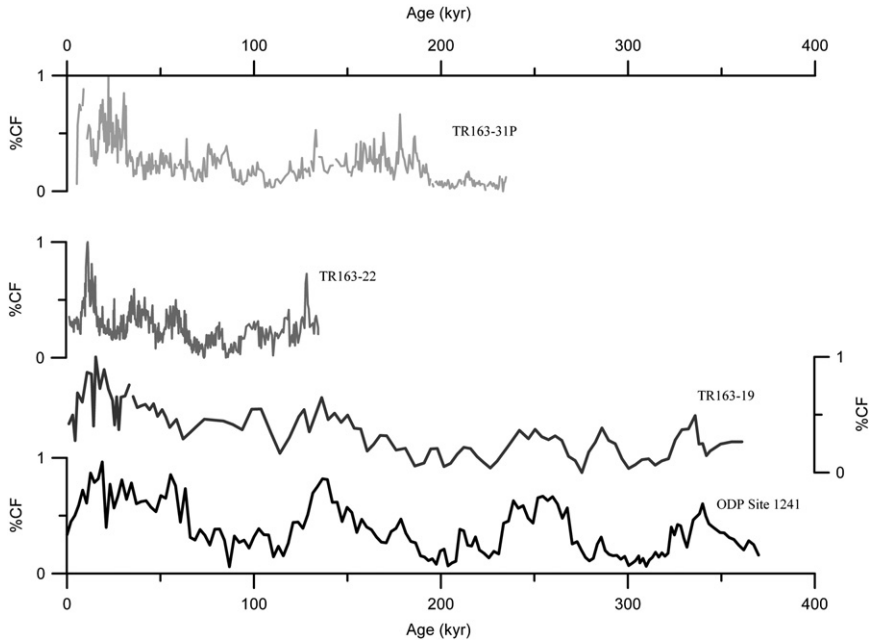

Fig. 8. Normalized %CF records from available EEP cores (all axes on the same scale): ODP Site 1241 (5°50.57′N, 86°26.676′W; 2027 m) (bottom), TR163-19 (2°15.5′N, 90°57.1′W; 2348 m) (bottom center) (Lea et al., 2000), TR163-22 (0°30.9′N, 92°23.9′W; 2830 m) (Lea et al., 2006), and TR163-31P (3°35′S, 83°57′W; 3205 m) (Martin et al., 2002). Normalized values demonstrate the similar magnitudes of the fluctuations in %CF between the four cores.

may have an overprint of export production on their dissolution proxies that could account for some of the difference between the records. This is an important observation that might explain the lack of relationship between the dissolution indices and the concentration of $CaCO_3$.

4.4. Carbonate dissolution in the equatorial Pacific

Both the ODP Site 1241% shell fragmentation and %CF records show a major dissolution event at the core-top, with values of 19% and 10% for fragmentation and %CF, respectively (Fig. 6). This late Holocene dissolution event has been seen in other cores from the WEP (Le and Shackleton, 1992), the central equatorial Pacific (Farrell and Prell, 1991), and the EEP (Lea et al., 2006; Ninkovich and Shackleton, 1975). The dissolution event has been predicted by models, which attempt to explain the changes in atmospheric pCO_2 during glacial and interglacial times (Boyle, 1988; Broecker, 1982; Keir and Berger, 1983). Preservation reaches its maximum at ~14 kyr in the fragmentation record and ~24 kyr in the %CF record before the Holocene dissolution pulse.

Comparing the ODP Site 1241%CF record to dissolution records from sites across the Pacific shows a clear common signal. Farrell and Prell (1991) reconstructed $\%CaCO_3$ isopleths from a suite of cores in the central equatorial Pacific (CEP). The changes in the %CF record from ODP Site 1241 have similar timings to the CEP dissolution patterns (Fig. 9). Slight variations do exist, most likely as a result of differences in the age models used to stratigraphically align each data set, as well as the respective resolution of each data set. This correlation between the two different proxies further supports the hypothesis that %CF is recording a basin-wide dissolution signal. Comparing the %CF record from ODP Site 1241 to a %CF record from western equatorial Pacific site ODP 806B (0°19.1′N, 159°21.7′E; 2520 m) (Medina-Elizalde, 2007) also demonstrates the Pacific basin-wide fluctuations in preservation (Fig. 10). The timings of the fluctuations are similar in both records, with noticeable preservation spikes at 14 and 130 kyr followed by a dissolution event at the core top. Cross-spectral analysis performed on dissolution proxies and $\delta^{18}O$ from the WEP and EEP indicate that both regions have a similar phase angle between dissolution and ice volume signal (Table 3). The magnitude of the %CF fluctuations is much greater in the WEP, which may be the result of different faunal assemblages inhabiting the relatively warm waters of the region. By examining the correlation of productivity indicators and dissolution proxies, Yasuda et al. (1993) suggested that productivity variations in the WEP played a subordinate role to carbonate dissolution fluctuations, and therefore the reasoning of Adelseck and Anderson (1978) cannot be used to explain the %CF changes in this region. Therefore dissolution patterns in the WEP are likely dominated by changes in bottom-water carbonate chemistry on glacial-to-interglacial time scales (Yasuda et al., 1993). Whereas the intensity of dissolution might have varied between regions, the synchronous timing of the fluctuations demonstrates that there were basin-wide changes in ocean chemistry occurring at glacial–interglacial transitions.

A number of hypotheses have been proposed to link dissolution fluctuations to atmospheric pCO_2 changes that occurred on glacial-to-

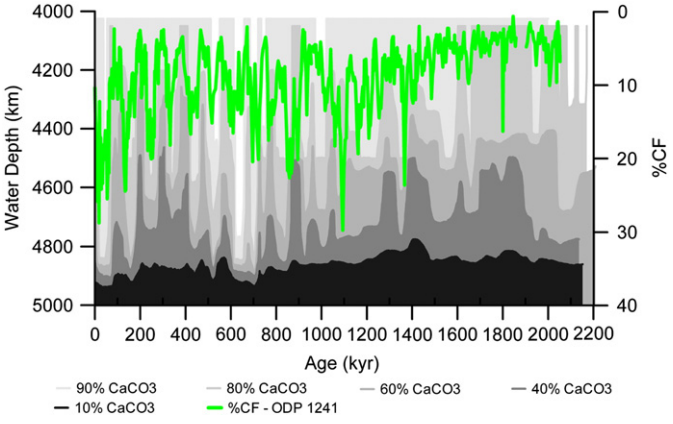

Fig. 9. Bathymetric variations in $\%CaCO_3$ from cores in the central equatorial Pacific (CEP) (Farrell and Prell, 1991) and the %CF record from ODP Site 1241 (5°50.57′N, 86°26.676′W). $\%CaCO_3$ measurements are contoured with 6 isopleths. The %CF axis is reversed so that up indicates increasing dissolution. During periods of intensified dissolution the $\%CaCO_3$ isopleths shoal indicating less carbonate at shallower depths. The timings of the dissolution fluctuations are similar in both the EEP %CF record and the CEP record. Some differences occur because of the ash deposits in the ODP Site 1241 record, a slight difference in the age models used to stratigraphically align both data sets, and data resolution differences. Figure modified from Farrell and Prell (1991).

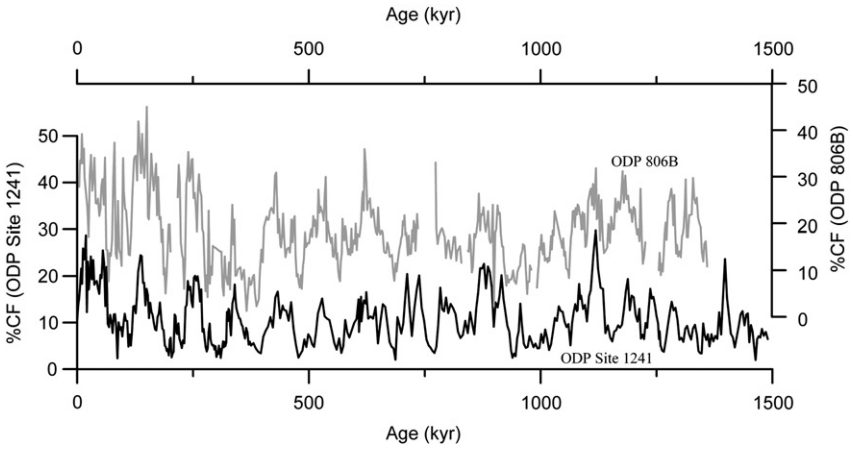

Fig. 10. ODP Site 1241 (5°50.57′N, 86°26.676′W; 2027 m) %CF record (bottom) in stratigraphic alignment with the ODP 806B (0°19.1′N, 159°21.7′E; 2520 m) (top) (Medina-Elizalde, 2007). The timings of the major dissolution fluctuations are in phase between the EEP and WEP. Overall cross correlation between the two records is r = 0.57.

interglacial timescales. Examining the $\delta^{18}O$, $\delta^{13}C$, and %CF records (Fig. 4) from ODP Site 1241 allows for a test of some of these hypotheses. At ODP Site 1241, $\delta^{13}C$ and $\delta^{18}O$ are in phase throughout the core (Table 3). During glacial maxima the $\delta^{13}C$ record shows the most isotopically negative values (Fig. 4). Cross-spectral analysis performed on the %CF and the $\delta^{18}O$ record show a linear correlation of r = 0.66 and a lag of preservation maxima to glacial maxima of 9–14 kyrs over the major orbital frequencies (Table 3). Preservation spikes occur roughly in the middle of the deglaciations, and dissolution becomes progressively stronger throughout the first half of the interglacial (Fig. 4). This is apparent in the record from 0 to 1300 kyr; before ~1300 kyr, the amplitude of the %CF cycles is considerably smaller. The increase in the amplitude of the %CF record occurs during the transition from the 41-kyr dominated $\delta^{18}O$ signal to the 100-kyr dominated $\delta^{18}O$ signal. The implication is that changes in carbon cycle feedbacks and ocean chemistry that occurred during the mid-Pleistocene transition influenced the dissolution signal (Clark et al., 2006; Kohler and Bintanja, 2008; Medina-Elizalde and Lea, 2005; Raymo et al., 1997). There are no published fragmentation or %CF records from other cores that extend back to ~2.1 Ma, so it is difficult to verify this hypothesis with other records.

The $\delta^{13}C$ signal in the Pacific has been interpreted as a record of changes in mean ocean carbon (Curry et al., 1988; Mix et al., 1995a,b; Shackleton, 1977). Shackleton (1977) suggested that rapid growth of the biosphere during deglaciation would result in extraction of CO_2 from the atmosphere–ocean system and ultimately cause enhanced carbonate preservation. This would be reflected in the $\delta^{13}C$ record as a positive excursion because isotopically negative CO_2 was being drawn out of the ocean (Shackleton, 1977). The isotopic evidence from ODP Site 1241 supports this view in that both the oxygen and carbon isotope signal are in phase and during deglaciations $\delta^{13}C$ values become increasingly positive. The %CF signal also records this effect because extraction of CO_2 from the ocean would result in less corrosive waters and enhanced preservation. Maximum preservation in the record occurs during deglaciations, lagging the ice volume and carbon signals by 9–14 kyr on the orbital frequencies, most likely as a result of the carbonate system response time (Archer, 1991; Le and Shackleton, 1992).

Although the Shackleton (1977) hypothesis is supported by the data from ODP Site 1241, the cause of the dissolution fluctuations is most likely the result of a combination of processes occurring at the transition from the glacial to interglacial intervals. For example, another model proposed that changes in the exchange of CO_2 into and

Table 3
Results of cross-spectral analysis.

Core	X,Y	100 kyr			41 kyr			23 kyr		
		Phase		Coherency[a,b]	Phase		Coherency[a,b]	Phase		Coherency[a]
		Phase angle (°)	kyr		Phase angle (°)	kyr		Phase angle (°)	kyr	
ODP 1241 (0 − .9 Ma)	δ180, %CF	52 ± 10	14.4 ± 3	0.97	87 ± 22	9.7 ± 2	0.87	139 ± 39	8.9 ± 2.5	0.67[c]
ODP 1241 (.9 − 2 Ma)	δ180, %CF	NA	NA	NA	127 ± 24	14.1 ± 2.6	0.86	163 ± 27	10.6 ± 1.7	0.82
ODP 1241[d]	δ180, δ13C	−18 ± 17	−4.9 ± 5	0.92	11 ± 14	1.3 ± 1.7	0.94	−34 ± 28	−2.2 ± 1.9	0.81[b]
ODP 1241 (0 − .9 Ma)	δ13C, %CF	76 ± 22	19 ± 5.6	0.87	84 ± 26	9.3 ± 3	0.82	NA	NA	NA
ODP 1241 (.9 − 2 Ma)	δ13C, %CF	56 ± 24	15.4 ± 6.5	0.86	114 ± 16	12.6 ± 1.8	0.93	98 ± 23	6.5 ± 1.5	0.86
ODP 806B[e,f]	δ180, %CF	58 ± 23	16.1 ± 6	0.75	92 ± 16	10.5 ± 2	0.93	150 ± 18	9.6 ± 1	0.92[c]
RC17-177[g,h]	δ180, % Frag	77 ± 123	21.4 ± 4	0.96	85 ± 40	9.7 ± 5	0.68	115 ± 28	7.3 ± 2	0.85
V28-238[g,h]	δ180, % Frag	56 ± 26	15.6 ± 7	0.87	106 ± 22	12.1 ± 3	0.90	143 ± 17	9.1 ± 1	0.67
ERDC-93P[g,h]	δ180, % Frag	58 ± 19	16.1 ± 5	0.92	128 ± 41	35.6 ± 11	0.69	133 ± 24	8.5 ± 2	0.88

NA: indicates no confidence.
[a] Coherency reported as r value.
[b] Correlation is significant at the 95% confidence interval.
[c] Correlation is significant at the 80% confidence interval.
[d] 0-1900 kyr time interval.
[e] 0-1400 kyr time interval.
[f] 0-500 kyr time interval.
[g] (Medina-Elizalde, 1992).
[h] (Le and Shackleton, 1992).

out of the ocean during glacial to interglacial transitions could be caused by strengthening of the southern overturning circulation due to a positive feedback that involves the position of the westerly winds (Toggweiler et al., 2006). The data from ODP Site 1241 supports this model, with a positive shift in $\delta^{13}C$ during deglaciations (indicating venting of respired CO_2) and the related increase in preservation. Both the terrestrial carbon sink model of Shackleton (1977) and the recently proposed model by Toggweiler et al. (2006) can explain the patterns of $\delta^{13}C$ and preservation in the ODP Site 1241 record, although it remains difficult to separate the two signals in the carbon isotope record.

5. Conclusions

A stable isotope record from ODP Site 1241 indicates that the top 45 m represents ~2.1 Ma of continuous sedimentation. A record of percentage coarse fraction from ODP Site 1241 demonstrates a basin-wide dissolution signal; this record displays similar phase lags relative to oxygen isotopes as is seen for dissolution proxies in the WEP. The preservation at ODP Site 1241 is slightly poorer than that of a slightly deeper Cocos Ridge core, TR163-19, most likely due to differences in sedimentation rates. Normalized %CF records from the EEP show similar timings and magnitudes in the major dissolution events between shallow- and deep-water cores. A comparison of WEP and EEP dissolution records shows a similar correlation for the timings of the events, but with a much greater magnitude in the fluctuations of the WEP. Since productivity has not varied much in the WEP (Yasuda et al., 1993), changes in bottom water carbonate saturation state must be responsible for the observed signal. The %CF record from ODP Site 1241 documents one of the first dissolution records to extend back to ~2.1 Ma. A remarkable increase in amplitude of the signal occurs at the mid-Pleistocene transition, perhaps related to changes in the global carbon system that forced climate from a 41-kyr to a 100-kyr dominated climate system (Clark et al., 2006; Kohler and Bintanja, 2008; Medina-Elizalde and Lea, 2005). The dissolution fluctuations and $\delta^{13}C$ signal observed at ODP Site 1241 are consistent with both the Shackleton (1977) and Toggweiler et al. (2006) models that explain changes in the global carbon signal. The lag between %CF and the $\delta^{13}C$ and ice volume records most likely reflects the response time for the ocean carbonate system.

Acknowledgements

We thank the ODP and ODP Leg 202 crew for gathering and providing the sample material, G. Paradis and H. Berg for stable isotope mass spectrometer operation and technical support (UCSB), Jenny King and Leah Carver for assistance with sample preparation (UCSB), Sarah Medley, Kate Steger, LiLing Hamady and Martin Medina-Elizalde for lab support (UCSB), James Kennett, Susannah Porter, and Jordan Clark for comments on the research (UCSB), and Rick Murray for his constructive reviews of the manuscript. This work has been previously defended and accepted for a MS degree at the University of California, Santa Barbara under the guidance of Dr. David W. Lea. This material is based upon work supported by the National Science Foundation under Grant no. OCE 0602362.

References

Adelseck Jr., C.G., Anderson, T.F., 1978. The late Pleistocene record of productivity fluctuations in the eastern equatorial Pacific Ocean. Geology 6 (7), 388–391.
Anderson, R.F., Fleisher, M.Q., Lao, Y., Winckler, G., 2008. Modern CaCO3 preservation in equatorial Pacific sediments in the context of late-Pleistocene glacial cycles. Mar. Chem. 111, 30–46.
Archer, D., 1991. Equatorial Pacific calcite preservation cycles: production or dissolution? Paleoceanography 6 (5), 561–571.
Arrhenius, G., 1952. Sediment cores from the east Pacific. Reports of the Swedish Deep Sea Expedition, 5, pp. 1–202. 1947–1948.
Arrhenius, G., 1988. Rate of production, dissolution and accumulation of biogenic solids in the ocean. Palaeogeogr. Palaeoclimatol. Palaeoecol. 67 (1–2), 119–146.
Bassinot, F.C., Beaufort, L., Vincent, E., Labeyrie, L., Rostek, F., Muller, P., Quidelleur, X., Lancelot, Y., 1994. Coarse fraction fluctuations in pelagic carbonate sediments from the tropical Indian Ocean: a 1500-kyr record of carbonate dissolution. Paleoceanography 9 (4), 579–600.
Berelson, W.M., Hammond, D.E., Cutter, G.A., 1990. In situ measurements of calcium carbonate dissolution rates in deep-sea sediments. Geochim. Cosmochim. Acta 54 (11), 3013–3020.
Berger, W.H., 1970. Planktonic Foraminifera — selective solution and the lysocline. Mar. Geol. 8 (2), 111–138.
Berger, W.H., 1973. Deep-sea carbonates: Pleistocene dissolution cycles. J. Foramin. Res. 3, 187–195.
Berger, W.H., 1977. Deep-sea carbonate and the deglaciation preservation spike in pteropods and foraminifera. Nature 269, 301–304.
Berger, W.H., Johnson, T.C., 1976. Deep-sea carbonates: dissolution and mass wasting on Ontong-Java Plateau. Science 192 (4241), 785–787.
Boyle, E.A., 1988. The role of vertical chemical fractionation in controlling the late Quaternary atmospheric carbon dioxide. J. Geophys. Res. 93, 701–715.
Broecker, W.S., 1982. Glacial to interglacial changes in ocean chemistry. Prog. Oceanogr. 11 (2), 151–197.
Broecker, W.S., Peng, T.H., 1987. The role of CaCO3 compensation in glacial to interglacial atmospheric CO2 change. Glob. Biogeochem. Cycles 1, 15–19.
Clark, P.U., Archer, D., Pollard, D., Blum, J.D., Rial, J.A., Brovkin, V., Mix, A.C., Pisias, N.G., Roy, M., 2006. The middle Pleistocene transition: characteristics, mechanisms, and implications for long-term changes in atmospheric pCO2. Quatern. Sci. Rev. 25 (23–24), 3150–3184.
Curry, W.B., Duplessy, J.C., Labeyrie, L., Shackleton, N.J., 1988. Changes in the distribution of ∂13 C of deep water ∑CO2 between the last glaciation and the Holocene. Paleoceanography 3 (3), 317–341.
Farrell, J.W., Prell, W.L., 1991. Pacific CaCO3 preservation and ∂18O since 4 Ma: paleoceanic and paleoclimatic implications. Paleoceanography 6 (4), 485–498.
Howell, P., Pisias, N., Ballance, J., Baughman, J., Ochs, L., 2006. ARAND Time-Series Analysis Software. Providence, RI.
Karlin, R., Lyle, M., Zahn, R., 1992. Carbonate variations in the Northeast Pacific during the Late Quaternary. Paleoceanography 7 (1), 43–61.
Keir, R.S., Berger, W.H., 1983. Atmospheric CO_2 content in the last 120, 000 years: the phosphate-extraction model. J. Geophys. Res. 88, 6027–6038.
Kimoto, K., Takaoka, H., Oda, M., Ikehara, M., Matsuoka, H., Okada, M., Oba, T., Taira, A., 2003. Carbonate dissolution and planktonic foraminiferal assemblages observed in three piston cores collected above the lysocline in the western equatorial Pacific. Mar. Micropaleontol. 47, 227–251.
Kohler, P., Bintanja, R., 2008. The carbon cycle during the Mid Pleistocene Transition: the Southern Ocean Decoupling Hypothesis. Clim. Past 4, 311–332.
Ku, T.L., Oba, T., 1978. A method for the quantitative evaluation of carbonate dissolution in deep-sea sediments and its application to paleoceanographic reconstruction. Quatern. Res. 10, 112–129.
Lalicata, J.J., 2009. Pleistocene carbonate dissolution fluctuations in the eastern equatorial Pacific on glacial timescales. Unpublished MS thesis, University of California, Santa Barbara, Santa Barbara, 74 pp.
LaMontagne, R.W., Murray, R.W., Wei, K.-Y., Leinen, M., Wang, C.-H., 1996. Decoupling of carbonate preservation, carbonate concentration, and biogenic accumulation: a 400 k.y. record from the central equatorial Pacific Ocean. Paleoceanography 11, 553–562.
Le, J., Shackleton, N.J., 1992. Carbonate dissolution fluctuations in the western equatorial Pacific during the late Quaternary. Paleoceanography 7 (1), 21–42.
Lea, D.W., Pak, D.K., Spero, H.J., 2000. Climate impact of late quaternary equatorial pacific sea surface temperature variations. Science 289 (5485), 1719–1724.
Lea, D.W., Martin, P.A., Pak, D.K., Spero, H.J., 2002. Reconstructing a 350 ky history of sea level using planktonic Mg/Ca and oxygen isotope records from a Cocos Ridge core. Quatern. Sci. Rev. 21 (1–3), 283–293.
Lea, D.W., Pak, D.K., Belanger, C.L., Spero, H.J., Hall, M.A., Shackleton, N.J., 2006. Paleoclimate history of Galapagos surface waters over the last 135, 000 yr. Quatern. Sci. Rev. 25 (11–12), 1152–1167.
Lisiecki, L.E., Lisiecki, P.A., 2002. Application of dynamic programming to the correlation of paleoclimate records. Paleoceanography 17 (4), 1049. doi:10.1029/2001PA000733.
Lisiecki, L.E., Raymo, M.E., 2005. A Pliocene–Pleistocene stack of 57 globally distributed benthic ∂18O records. Paleoceanography 20 (1), PA1003.
López-Otálvaro, G.-E., Flores, J.-A., Sierro, F.J., Cacho, I., 2008. Variations in coccolithophorid production in the Eastern Equatorial Pacific at ODP Site 1240 over the last seven glacial–interglacial cycles. Mar. Micropaleontol. 69 (1), 52–69.
Luz, B., Shackleton, N.J., 1975. CaCO3 solution in the tropical east Pacific during the past 130, 000 years. Spec. Publ. Cushman Found. Foramineferal. Res. 13, 4824–4841.
Martin, P.A., Lea, D.W., Rosenthal, Y., Shackleton, N.J., Sarnthein, M., Papenfuss, T., 2002. Quaternary deep sea temperature histories derived from benthic foraminiferal Mg/Ca. Earth Planet. Sci. Lett. 198 (1–2), 193–209.
Matsuoka, H., 1990. A new method to evaluate dissolution of CaCO3 in deep-sea sediments. Trans. Proc. Paleontol. Soc. Jpn. 157, 430–434 N.S..
Medina-Elizalde, M., 2007. The Thermal Evolution of the Western Equatorial Pacific Warm Pool During the Pleistocene and Late Pliocene Epochs. Unpublished PhD dissertation, University of California, Santa Barbara, Santa Barbara, 167 pp.
Medina-Elizalde, M., Lea, D.W., 2005. The mid-Pleistocene transition in the tropical Pacific. Science 310 (5750), 1009–1012.
Mix, A.C., Le, J., Shackleton, N.J., 1995a. Benthic foraminiferal stable isotope stratigraphy of Site 846: 0–1.8 Ma. Proc. ODP, Sci. Results, 138. Ocean Drilling Program, College Station, TX, pp. 839–854.
Mix, A.C., Pisias, N., Rugh, W., 1995b. Benthic foraminiferal stable isotope record from Site 849 (0–5 Ma). Proc. ODP, Sci. Results, 138. Ocean Drilling Program, College Station, TX, pp. 371–412.

Mix, A.C., Tiedemann, R., Blum, P., Abrantes, F.F., Benway, H., 2003. Site 1241. Proc. ODP Init. Results 202, 1–101.
Moore, T.C., Pisias, N.G., Heath, G.R., 1977. Climate changes and lags in the Pacific carbonate preservation, sea surface temperature, and global ice volumes. In: Andersen, N.R., Malahoff, A. (Eds.), The Fate of Fossil Fuel CO2 in the Oceans. Plenum, New York, pp. 145–166.
Murray, R.W., Knowlton, C., Leinen, M., Mix, A.C., Polsky, C.H., 2000. Export production and carbonate dissolution in the central equatorial Pacific Ocean over the past 1 Ma. Paleoceanography 15, 570–592.
Ninkovich, D., Shackleton, N.J., 1975. Distribution, stratigraphic position and age of ash layer "L", in the Panama Basin region. Earth Planet. Sci. Lett. 27 (1), 20–34.
Paytan, A., Kastner, M., Chavez, F.P., 1996. Glacial to interglacial fluctuations in productivity in the equatorial Pacific as indicated by marine barite. Science 274 (5291), 1355–1357.
Pedersen, T.F., 1983. Increased productivity in the eastern equatorial Pacific during the last glacial maximum (19, 000 to 14, 000 yr B.P). Geology 11 (1), 16–19.
Peterson, L.C., Prell, W.L., 1985. Carbonate dissolution in recent sediments of the eastern equatorial Indian Ocean — preservation patterns and carbonate loss above the lysocline. Mar. Geol. 64 (3–4), 259–290.
Pisias, N., 1976. Late Quaternary sediments of the Panama Basin: sedimentation rates, periodicities, and controls of carbonate and opal accumulation. Mem. Geol. Soc. Am. 145, 375–392.
Raymo, M.E., Oppo, D.W., Curry, W.B., 1997. The mid-Pleistocene climate transition: a deep sea carbon isotopic perspective. Paleoceanography 12 (4), 546–559.
Reynolds, R.W., Rayner, N.A., Smith, T.M., Stokes, D.C., Wang, W., 2002. An Improved In Situ and Satellite SST Analysis for Climate. J. Climate 15, 1609–1625.
Shackleton, N.J., 1977. Carbon-13 in *Uvigerina*: tropical rain forest history and the equatorial Pacific carbonate dissolution cycle. In: Andersen, N.R., Malahoff, A. (Eds.), The Fate of Fossil Fuel CO2 in the Oceans. Plenum, New York, pp. 401–427.
Shackleton, N.J., Hall, M.A., 1984. Oxygen and carbon isotope stratigraphy of Deep Sea Drilling Project Hole 552A: Plio-Pleistocene glacial history. Initial Rep. of the Deep Sea Drill. Proj. 81, 599–610.
Thompson, P.R., Saito, T., 1974. Pacific Pleistocene sediments: planktonic Foraminifera dissolution cycles and geochronology. Geology 2 (7), 333–335.
Thunell, R.C., Keir, R.S., Honjo, S., 1981. Calcite dissolution—an in situ study in the Panama Basin. Science 212, 659–661.
Toggweiler, J.R., Russell, J.L., Carson, S.R., 2006. Midlatitude westerlies, atmospheric CO2, and climate change during the ice ages. Paleoceanography 21 PA2005.
Vincent, E., Berger, W.H., 1981. Planktonic foraminifera and their use in paleoceanography. In: Emiliani, C. (Ed.), The Sea. : The Oceanic Lithosphere, Volume 7. John Wiley, New York, pp. 1024–1119.
Volat, J.L., Pastouret, L., Vergnaudgrazzini, C., 1980. Dissolution and carbonate fluctuations in Pleistocene deep-sea cores — a review. Mar. Geol. 34 (1–2), 1–28.
Yasuda, M., Berger, W.H., Wu, G., Burke, S., Schmidt, H., 1993. Foraminifer preservation record for the last million years: Site 805, Ontong Java Plateau. Proc. Ocean Drill. Program Sci. Results 130, 491–508.